

Notat: Utredning av høye rekkverk på Askøybrua

Vedlegg 5:

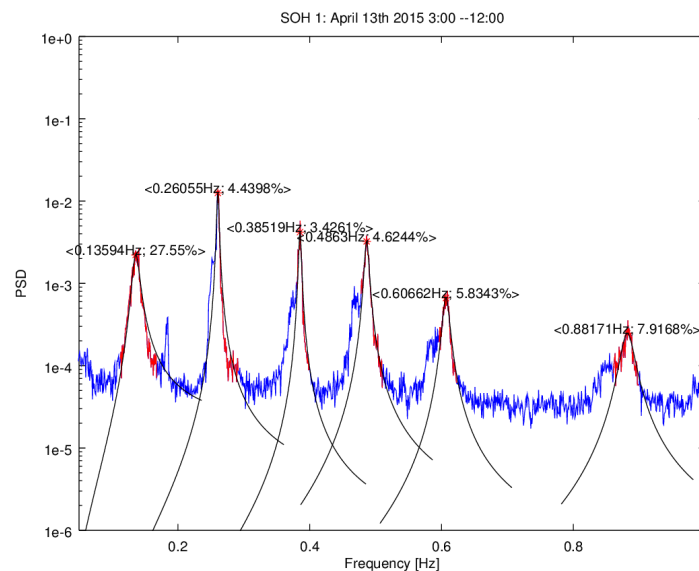
Rapport: Askøy bridge, In-situ measurements. 21.05.2015.

Svend Ole Hansen APS.



STRUCTURAL DAMPING OF THE ASKØY BRIDGE

In-situ measurements of natural frequencies and dampings



Prepared for: Statens Vegvesen

Revision 0, 2015



Contents

0	Summary and conclusion	3
1	Introduction	6
2	Measurements	7
3	Aerodynamic Damping	8
4	Results and discussion	9
	References	16

Revisions

Revision	Date	Note
DRAFT	April 17, 2015	Draft report, issued for comments.
DRAFT	May 16, 2015	Draft including higher-order vertical modes. Issued for comments.
Rev. 0	May 20, 2015	Final report.
Rev. 1	May 21, 2015	Corrected sign of δ_a . Minor editorial edits.



0 Summary and conclusion

The purpose of the present report, which is prepared for Statens Vegvesen in Norway, is to identify, by in-situ measurements, the natural frequencies and associated structural dampings of the Askøy Bridge. The lowest-order heave and torsion modes are of main interest. This investigation was initiated in order to determine whether a planned modification of walkways and bridge railings makes the bridge susceptible to vortex-induced vibrations (see our previous report [1]). The wind tunnel tests of ref. [1] showed that the current bridge is not susceptible to vortex-induced vibrations for logarithmic damping decrements above approx. 3.6 % for heaving vibrations and 1.8 % for torsional vibrations.

Vibration measurements are carried out continuously by eight mobile phones mounted on the Askøy bridge. Vibrations are registered by their internal 3-dimensional DC accelerometers. The system was implemented on March 27, 2015. The data providing the basis for this memo was recorded at dates specified in Table 0.1. Figure 0.1 shows the wind directions relative to the bridge. The wind data is taken from NMI at the Flesland measuring station.

Table 0.1. Dates of measurements.

Date	Mean wind [m/s]	Direction [°]
March 28th 2015 7:00–15:00	11.0	152
April 7th 2015 1:00–9:00	3.3	265
April 13th 2015 3:00–12:00	5.9	331

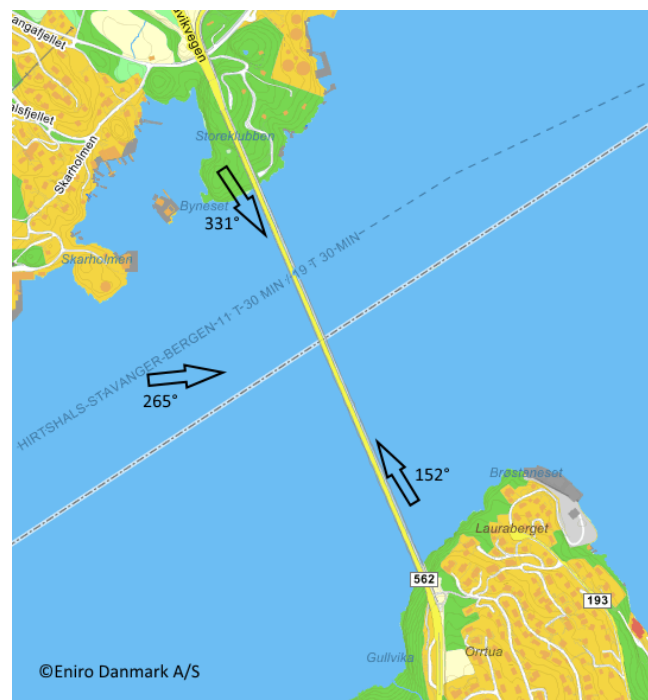


Figure 0.1. The three investigated wind directions plotted relative to the bridge.



The natural frequencies and associated structural dampings of the identified lowest-order vibration modes are summarised in Table 0.2.

Table 0.2. Damping estimates at different wind conditions.

Mode	Wind		Frequency [Hz]	Damping decrement	
	Mean [m/s]	Direction [°]		Total [%]	Structural [%]
V1	3.3	265	0.137	>20	>20
V1	5.9	331	0.136	>20	>20
V1	11.0	152	0.137	>20	>20
V2	3.3	265	0.182	1.3	2.3
V2	5.9	331	0.183	2.0	2.0
V2	11.0	152	0.183	2.8	2.8
V3	3.3	265	0.262	1.6	2.6
V3	5.9	331	0.261	4.4	4.4
V3	11.0	152	0.261	4.3	4.4
V5	3.3	265	0.384	3.2	3.2
V5	5.9	331	0.385	3.4	3.4
V5	11.0	152	0.382	4.4	4.4
V6	3.3	265	0.485	3.0	3.0
V6	5.9	331	0.486	4.6	4.6
V6	11.0	152	0.485	3.7	3.7
T1	3.3	265	0.603	3.7	3.7
T1	5.9	331	0.607	5.8	5.8
T1	11.0	152	-	-	-
T2	3.3	265	0.876	9.5	9.5
T2	5.9	331	0.882	7.9	7.9
T2	11.0	152	0.878	7.4	7.4

The measured natural frequencies of the first 6 vertical modes, except vertical mode V4, which was not clearly identified in the measured data, and of the first two torsional modes agree within approx. 4% with the natural frequencies determined by Norconsult in their theoretical FEM calculations.

The logarithmic damping decrement measured in the torsional vibrations are all larger than the minimum requirement of 1.8% indicating that the present bridge is not susceptible to vortex-induced torsional vibrations.

The logarithmic damping decrement determined in the vibrations of the second and third vertical modes, V2 and V3, are less than the minimum requirement of 3.6% indicating that the present bridge may experience vortex-induced vertical vibrations of these two modes.

For the remaining vertical modes, the structural damping determined is larger than the minimum requirement. The lowest structural damping of approx. 2% is determined for the second vertical mode V2 having a natural frequency of 0.183 Hz indicating that this mode



may be the most susceptible to vortex-induced vibrations. The findings above are in good agreement with the full-scale experience, indicating that vortex-induced vibrations actually may occur on the present bridge.

It is reassuring to experience this degree of agreement between section model testing and actual full-scale observations.

The uncertainty regarding risk of vortex-induced vibrations on future modified geometries of the Askøy bridge may be reduced to a minimum by measuring the bridge response to vortex-induced vibrations over a wide range of dampings, for the present configuration and modified configuration.

Copenhagen, May 20, 2015

Svend Ole Hansen ApS

Svend Ole Hansen

Project Engineer

Teis Schnipper

Project Engineer

Simon Merlung



1 Introduction

Askøy Bridge is an existing suspension-bridge connecting Askøy and Bergen across Byfjorden. The main span is 850 m. The cross-section consists of a simple 15.5 m wide composite deck.

Wind tunnel tests focusing on the aerodynamic stability of a suggested modification of the footpaths and fencing raised concern whether the bridge would be rendered susceptible to vortex-induced vibrations, see ref [1]. The wind tunnel tests showed that the bridge cross section is not susceptible to vertical vortex-induced vibrations for logarithmic damping decrements above approx. 3.6% for heaving vibrations and 1.8% for torsional vibrations.

This report presents in-situ measurements of the natural frequencies and structural dampings associated with the lowest-order vertical and torsional vibration modes. Bridge vibrations are excited by the natural wind, and to a lesser extend, traffic. Bridge vibrations are measured by a system of eight three-dimensional vibration transducers and one anemometer registering the wind speed and angle. The system was mounted on March 27 2015, and has been measuring continuously since (currently, 4000 hours of vibration data is obtained).



2 Measurements

Bridge vibrations are registered using eight stock mobile phones (Samsung Galaxy S4 Mini). Each unit is equipped with a MEMS-based DC accelerometer with a resolution of approx. 0.6 mm/s^2 . This corresponds to a vibration amplitude of 1.5 mm at 1 Hz. The scanning rate is approximately 80 Hz.

Bridge vibrations are measured continuously and data is stored in data files of ten-minute duration. At the time of writing, the measurements have generated approx. 4000 hours of vibration data.

In addition, the wind speed and angle was registered using a Gill Wind Master sonic anemometer placed close to the bridge's mid-span. Unfortunately, the anemometer data stream broke a few days after installation, presumably due to traffic disturbances.

2.1 Measurement positions

Measurement positions are shown in Fig. 2.1. Positions are marked with red text (sohNN), and black numbers refer to the girder box number, counting from Bergen. Wind is measured by "field003".

Measurement positions at girder box 54 and 160 are close to vibration-antinode of asymmetric modes, while girder box 107 is close to anti-nodes of most symmetric modes.

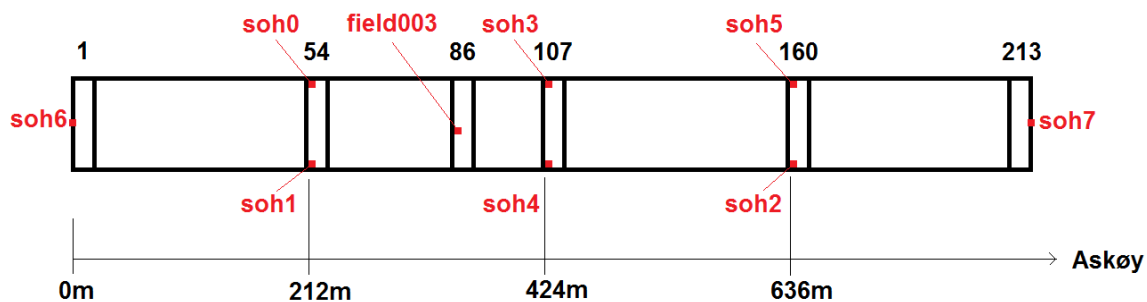


Figure 2.1. Measurement positions. Black numbers above the bridge refer to the box girder no. (counting from Bergen), and red text indicate measurement positions. The polyns are located at box girders 1 and 213, respectively.



3 Aerodynamic Damping

This chapter summarises the method used to determine the aerodynamic damping. The method is described in detail in ref. [3].

The measurements give rise to estimates of the total damping

$$\delta_t = \delta_a + \delta_s, \quad (3.1)$$

in which δ_s is the structural damping. The aerodynamic damping δ_a may be determined from the expression

$$\delta_a = -2\pi K_{aG} \frac{\rho h d}{m_e} \left(1 - \left(\frac{\sigma_y}{a_L h} \right)^2 \right), \quad (3.2)$$

in which K_{aG}, a_L are aerodynamic constants of the bridge, ρ is the air density, m_e is the effective linear density of the bridge, σ_y/h is the standard-deviation of the bridge vibration (due to VIV) nondimensionalised by the cross-wind bridge height h .

Table 3.1. Selected results from wind tunnel tests of the present bridge.

δ_t [%]	δ_s [%]	σ_y/h [-]
0.00	1.1	0.0368
0.69	2.5	0.0110

Selected results of wind tunnel tests focusing on VIV are given in Table 3.1. The data indicates an aerodynamic damping level of approx. $\delta_a = -1.8\%$ based on the test with $\delta_s = 2.5\%$. It is noted that the structural dampings listed above are estimated slightly higher than in ref. [1], for conservatism.

In the limit of negligible motion, the above estimate of aerodynamic damping yields the value $K_{aG} = 0.46$, which is rounded off to $K_{aG} = 0.5$. Using the bridge response at the low-damped case then yields the estimate $a_L = 0.056$, which is rounded off to $a_L = 0.06$.

The aerodynamic damping is then determined from Eq. (3.2), for all values of bridge motion levels, σ_y/h . The aerodynamic damping evaluated in this way is subtracted from the measured total damping.

Aerodynamic damping depends on the turbulence level in such a way that the vibration level becomes less with increasing turbulence. In order not to over-estimate the numerical value of the negative aerodynamic damping, a factor of 1/2 is applied to Eq. (3.2). That is, the aerodynamic damping (log. decrement) is evaluated as

$$\delta_a = -\pi K_{aG} \frac{\rho h d}{m_e} \left(1 - \left(\frac{\sigma_y}{a_L h} \right)^2 \right). \quad (3.3)$$

It is noted that a much more precise estimate of the aerodynamic damping may be obtained by measuring the bridge's VIV level over a wide range of dampings (Scruton numbers). This will reduce the uncertainty on predicted dampings of modified bridge cross sections to a minimum.



4 Results and discussion

4.1 Analysis

The traffic and wind loading is assumed to provide an excitation of the bridge which, within a certain range surrounding each natural frequency, is considered white-noise like.

The power spectral density (PSD) for each acceleration signal is determined, and random noise is removed by cutting the measured data into 20-minute samples and taking their averaged spectrum. The measurement time used in each position is approximately 8 hours. The spectrum peaks are then fitted with the acceleration frequency response function for the damped single-degree of freedom system

$$|H|_a^2 \propto \frac{\omega^4}{(\omega_0^2 - \omega^2)^2 + (2\zeta\omega_0\omega)^2} \quad (4.1)$$

using the damping ratio ζ and natural angular frequency $\omega_0 = 2\pi n_0$ where n_0 (the natural cyclic frequency in [Hz]) as fitting parameters. The fit makes use of an objective function which is evaluated as the residual 2-norm in frequency ranges relevant for the given peak.

4.2 Results

Vibration data from three different dates were used, see Table 4.1. The wind conditions correspond to moderate and significant winds (bridge parallel, no negative aerodynamic damping), wind perpendicular to the bridge (giving rise to negative aerodynamic damping for V1-V3 modes).

Table 4.1. Dates of measurements.

Date	Mean wind [m/s]	Direction [°]
March 28th 2015 7:00–15:00	11.0	152
April 7th 2015 1:00–9:00	3.3	265
April 13th 2015 3:00–12:00	5.9	331

Table 4.2 summarise the measured natural frequencies and their associated damping estimates, in terms of the logarithmic decrement LD , which is linked to ζ through

$$LD = \frac{2\pi\zeta}{\sqrt{1 - \zeta^2}} \quad (4.2)$$



Table 4.2. Damping estimates at different wind conditions.

Mode	Wind		Frequency [Hz]	Damping decrement	
	Mean [m/s]	Direction [°]		Total [%]	Structural [%]
V1	3.3	265	0.137	>20	>20
V1	5.9	331	0.136	>20	>20
V1	11.0	152	0.137	>20	>20
V2	3.3	265	0.182	1.3	2.3
V2	5.9	331	0.183	2.0	2.0
V2	11.0	152	0.183	2.8	2.8
V3	3.3	265	0.262	1.6	2.6
V3	5.9	331	0.261	4.4	4.4
V3	11.0	152	0.261	4.3	4.4
V5	3.3	265	0.384	3.2	3.2
V5	5.9	331	0.385	3.4	3.4
V5	11.0	152	0.382	4.4	4.4
V6	3.3	265	0.485	3.0	3.0
V6	5.9	331	0.486	4.6	4.6
V6	11.0	152	0.485	3.7	3.7
T1	3.3	265	0.603	3.7	3.7
T1	5.9	331	0.607	5.8	5.8
T1	11.0	152	-	-	-
T2	3.3	265	0.876	9.5	9.5
T2	5.9	331	0.882	7.9	7.9
T2	11.0	152	0.878	7.4	7.4

Wind conditions giving rise to accurate measurements of torsional mode shape T3 have not been identified. Also, vertical mode 4 is not giving identifiable from the spectras - this is presumably because this mode has vibration nodes very close to the midpoint, and quarter points, cf. Fig. 4.7.

Figures 4.1–4.6 show the PSDs measured. In all figures, blue curves show PSD and the black curves are fitting curves used to determine the frequency and damping. The frequency interval used for the fitting procedures cover the red spectrum segments. Note that some subjective filtration is used in cases where the peak is not quite symmetric. A conservative frequency band has been used here.

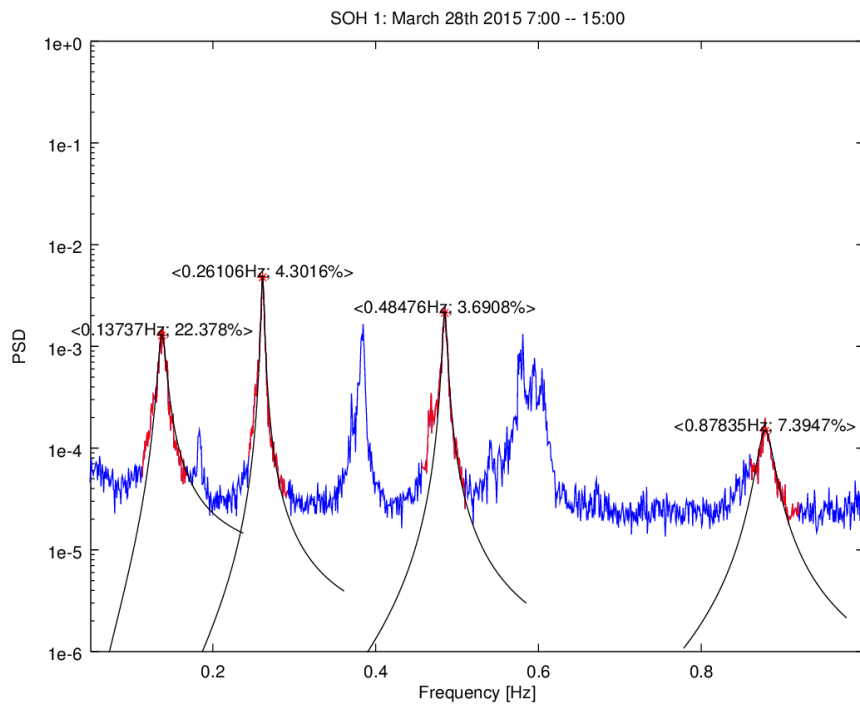


Figure 4.1. Spectrum measured by SOH1 in quarter point at March 28th

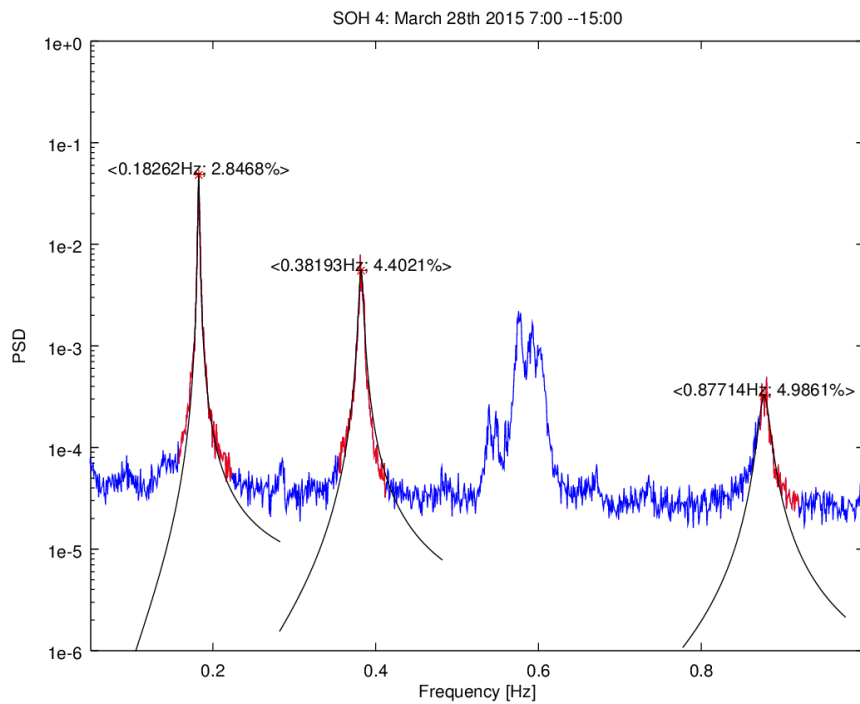


Figure 4.2. Spectrum measured by SOH4 in middle point at March 28th

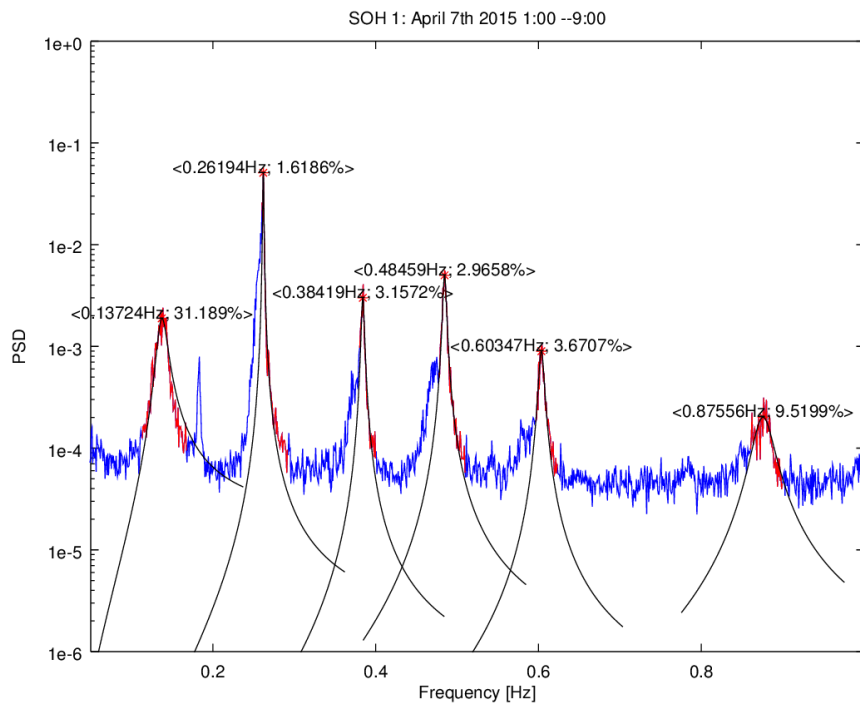


Figure 4.3. Spectrum measured by SOH1 in quarter point at April 7th

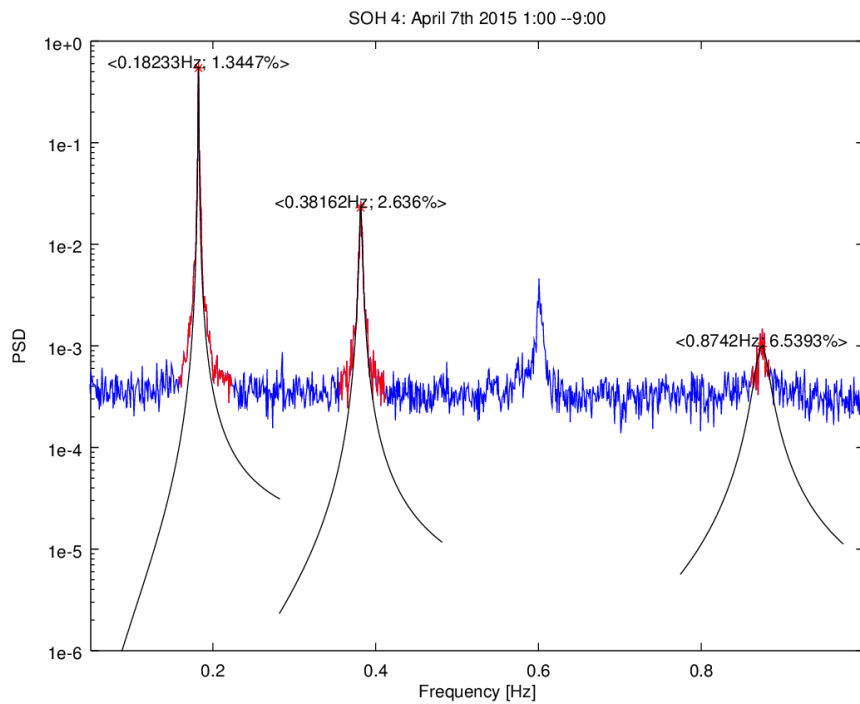


Figure 4.4. Spectrum measured by SOH4 in middle point at April 7th

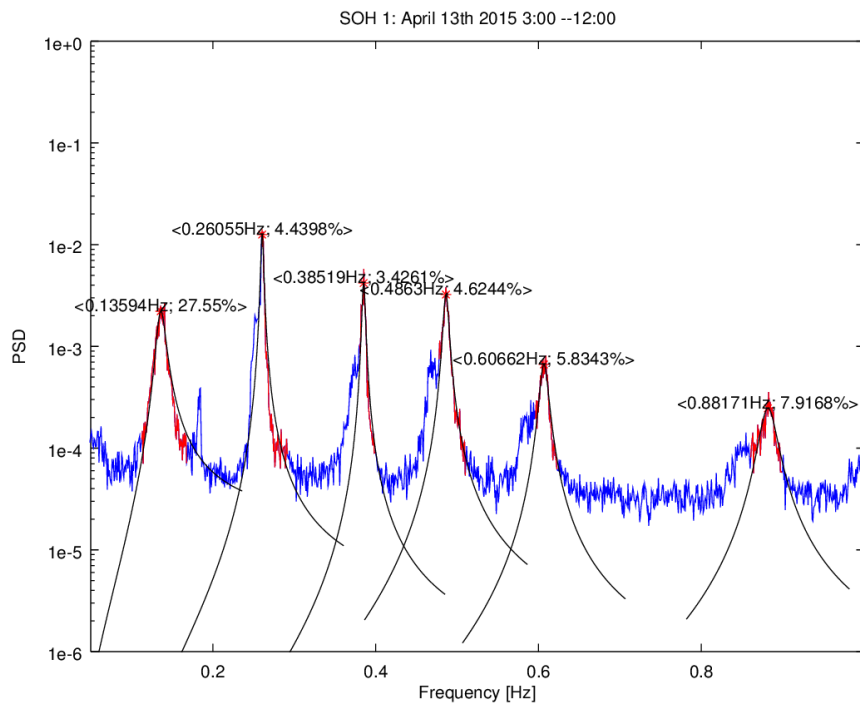


Figure 4.5. Spectrum measured by SOH1 in quarter point at April 13th

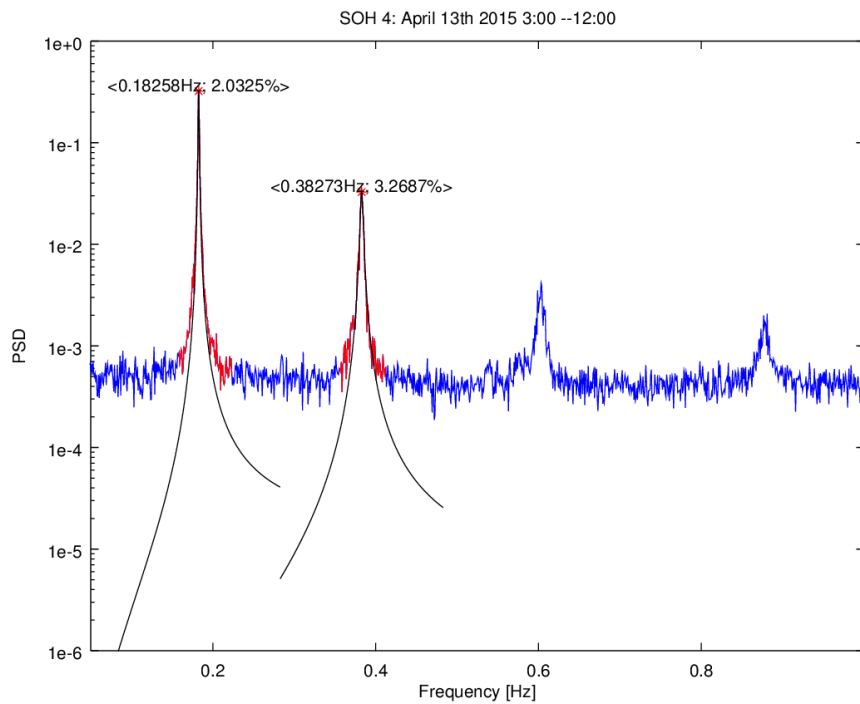


Figure 4.6. Spectrum measured by SOH4 in middle point at April 13th



4.3 Comparison with FE analysis

Mode shapes determined by Finite Element Analysis (FEA) have been supplied by Norconsult, see ref. [2]. Table 4.3. Summarises the comparison between the oscillation periods of the measured and predicted mode shapes, respectively.

Table 4.3. Comparison of the measured period ($T = f^{-1}$) with FEA predictions, cf. ref. [2].

Mode	Period, T [s]		
	Measured	FEA	Ratio
V1	7.31	7.04	96%
V2	5.48	5.41	98%
V3	3.85	3.83	99%
V4	-	3.47	-
V5	2.60	2.58	99%
V6	2.06	2.03	99%
T1	1.65	1.74	105%
T2	1.14	1.13	99%
T3	-	0.75	-

Figures 4.7–4.8 shows the mode shapes as determined by FEA.

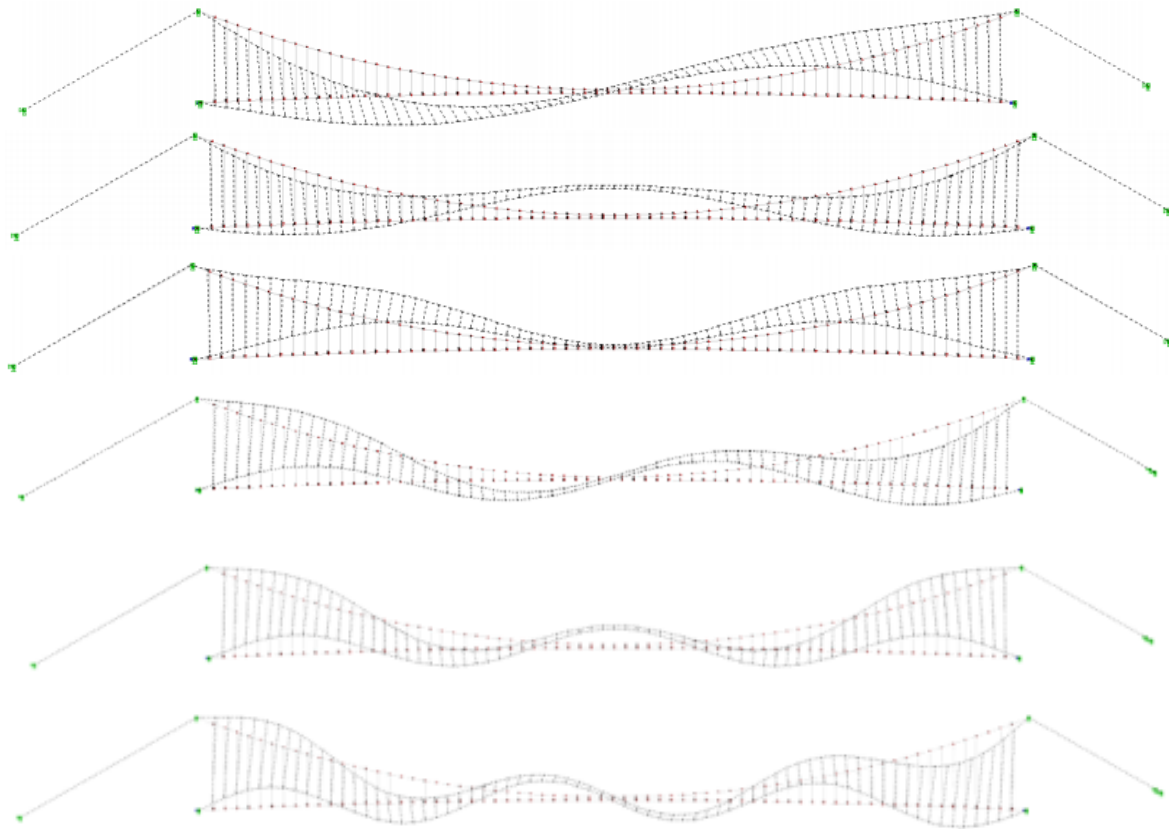


Figure 4.7. Vertical mode shapes V1 (top) to V6 (bottom).

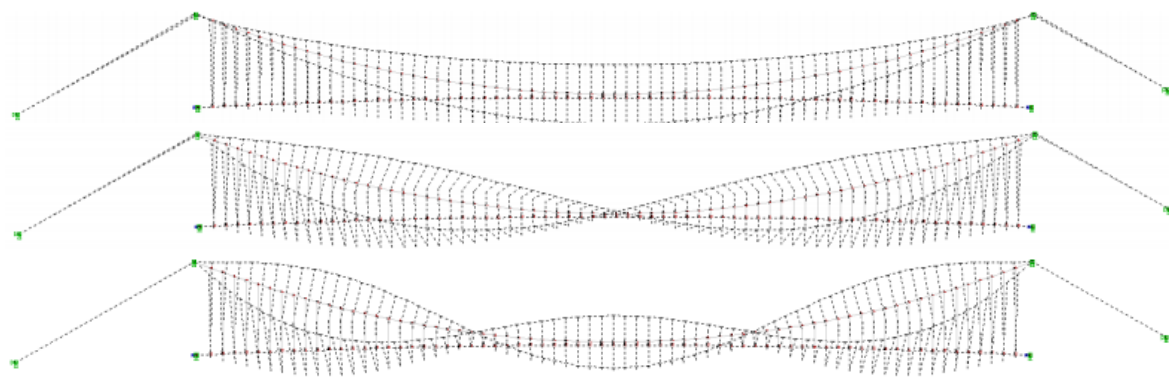


Figure 4.8. Torsional mode shape T1 (top) to T3 (bottom).



References

- [1] SOH report: *Askøy bridge - Wind tunnel tests and analyses*. Revision 0, December 2014.
- [2] Norconsult report: *Gangbane Askøybrua*. Revision 3, October 2014.
- [3] S. O. Hansen: *Vortex-induced vibrations – The Scruton number revisited*. Proceedings of the ICE – Structures and buildings **66**, Issue 10 (2013).